Available online at www.sciencedirect.com
ScienceDirect
Nuclear Instruments and Methods in Physics Research A 577 (2007) 381–385
NUCLEAR INSTRUMENTS & METHODS IN PHYSICS RESEARCH Section A
www.elsevier.com/locate/nima

Firsov approach to heavy-ion stopping in warm matter using a finite-temperature Thomas–Fermi model

Y. Oguri[a,*], T. Niinou[a], S. Nishinomiya[a], K. Katagiri[a], J. Kaneko[b], J. Hasegawa[a], M. Ogawa[a]

[a] Research Laboratory for Nuclear Reactors, Tokyo Institute of Technology, O-okayama 2-12-1-N1-14, Meguro-ku, 152-8550 Tokyo, Japan
[b] Faculty of Health Sciences, Komazawa University, Komazawa 1-23-1, Setagaya-ku, 154-8525 Tokyo, Japan

Available online 11 February 2007

Abstract

Low-velocity ($<c/137$) heavy-ion stopping in warm ($kT<10\,\mathrm{eV}$) matter was investigated by means of a Firsov model, in which the projectile energy loss was evaluated from the drag force due to the exchange of electrons between the projectile and the target. A finite-temperature Thomas–Fermi model was applied in order to calculate the density and momentum distribution of electrons around the nuclei of the collision partners. We have found that the stopping cross-section depends only weakly on the target temperature, whereas the density dependence is rather strong.

PACS: 31.15.Bs; 34.50.Bw; 52.27.Gr; 52.40.Mj

Keywords: Heavy ion inertial fusion; Plasma; Warm dense matter; Stopping power; Firsov model; Thomas–Fermi model

1. Introduction

Pulsed intense heavy-ion beams developed for inertial fusion have been recently recognized as one of the options to produce warm dense matter (WDM) in laboratories [1]. Homogeneous and efficient heating of solid targets with a finite thickness is foreseen using "Bragg peak" of the energy deposition profile. If a thicker target is used, one has to pay attention also to the stopping at lower velocities for detailed analysis of the end-of-range regions.

Ionization degree of warm matter is generally small. So far projectile stopping in such weakly-ionized plasmas, or materials consisting of excited atoms has been theoretically investigated [2–5]. In these studies, the projectile energies are high enough to apply the Bethe stopping scheme. On the other hand, there exist only few studies on the stopping of low-energy ($<100\,\mathrm{keV}$) heavy projectiles in plasmas [6,7]. In these studies, however, the densities of the target plasmas are much lower than those of WDM.

For projectiles slower than the Bohr velocity $v_B \equiv c/137$, the Bethe stopping scheme is not valid even for outermost orbital electrons in the target. Also the projectile charge is very small and not so definite owing to strong electron-exchange reactions between collision partners. In this case, the decelerating force onto the projectile is frictional and the stopping power is proportional to the projectile velocity. The energy loss mechanism of such low-energy projectiles due to the momentum transfer by electron exchange has been first proposed by Firsov [8]. In this approach, one has to determine the density and velocity distributions of electrons in both the projectile and the target atom, which form a quasi-molecule during the collision. In Firsov's original paper, a simple Thomas–Fermi estimate has been used to evaluate these distributions. By using more detailed atomic wave functions, for instance, Z_1 structures of experimental results have been successfully reproduced [9]. However, if the stopping medium is warm, one has to take into account not only the ground state but also all of the possible excited states. Also, if a dense target is used, deformation of atomic wave functions due to the decrease of the internuclear distance has to be included. Additionally, contributions of free

*Corresponding author. Tel.: +81 3 5734 3071; fax: +81 3 5734 2959.
E-mail address: yoguri@nr.titech.ac.jp (Y. Oguri).

0168-9002/$ - see front matter
doi:10.1016/j.nima.2007.02.009

electrons should be accommodated. These procedures are sometimes tedious at least for rough estimations. Thus, for warm dense targets, one may come back to statistical approaches such as a finite-temperature Thomas–Fermi model [10].

In this paper, we introduce a modified Firsov model, in which the electron exchange flux between the collision partners is calculated by using a finite-temperature Thomas–Fermi model applied to a mixture of excited atoms and some free electrons. The target temperature and density dependence of the stopping cross-section are investigated.

2. Method of calculation

2.1. Stopping power calculation by a Firsov model

The geometry used for the calculation is shown in Fig. 1. For each trajectory C(b) with an impact parameter b, the energy transferred from the projectile to the target by electron exchange is

$$\varepsilon(b) = m \int_{C(b)} \Phi(R) \frac{dR}{dt}\, dR = m \int_{C(b)} \Phi(R) v_p\, dR, \tag{1}$$

where m and $\boldsymbol{v}_p$ are the electron mass and the projectile velocity, respectively. The vector $\boldsymbol{R}$ is the internuclear distance between the projectile and the target. The electron flux through the "Firsov plane" A($\boldsymbol{R}$) is denoted by $\Phi(\boldsymbol{R})$. If we assume a spherical symmetry around each nucleus, the electron flux from one atom to the other is approximated by

$$\Phi(R) \approx \int_{A(R)} \frac{1}{4} n_e(r) v_e(r)\, dA, \tag{2}$$

where $n_e(r)$ and $v_e(r)$ are the electron-density and the averaged electron-velocity distribution in the radial coordinate r in one atom, respectively. Contributions of both the projectile and the target atoms must be added in the evaluation of Eq. (2). The position of the Firsov plane was determined using Kishenevsky's formula [11].

Stopping by free electrons are not treated by the original Firsov model. However, not only bound electrons, but also low-energy free electrons around the target atom can be captured by the projectile, if the total energy of a free

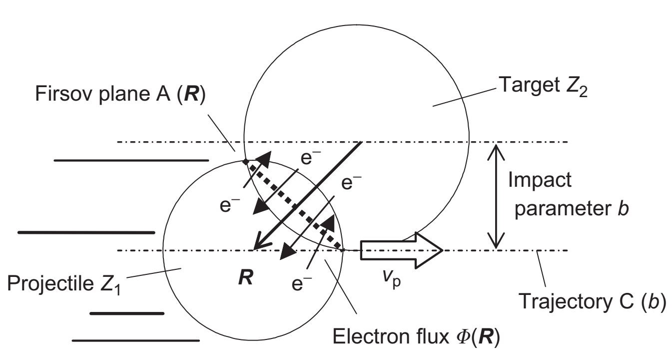

Fig. 1. Geometry for the stopping calculation by the Firsov model.

electron on the Firsov plane seen by the projectile is negative. Also the capture of free electrons around the projectile by the target atom is possible in a similar manner. Thus, contributions of such low-energy free electrons have been included in Eq. (2).

The stopping cross-section is obtained by summing up contributions of all possible trajectories with different impact parameters

$$S = \int_{b_0}^{\infty} 2\pi b \varepsilon(b)\, db. \tag{3}$$

The minimum impact parameter b_0 in the equation above was determined by an analytical method [9] from the setup geometry of the energy loss measurement. We assumed that the target mass thickness is always $10\,\mu g/cm^2$. A particle detector for the energy loss measurement was placed 1 m behind the target. The diameter of the sensitive area of the detector is 1 cm.

Now the problem is reduced to the evaluation of $n_e(r)$ and $v_e(r)$ for the projectile and the target atom on the Firsov plane.

2.2. Finite-temperature Thomas–Fermi model

Calculation of $n_e(r)$ and $v_e(r)$ was performed using a FORTRAN program [12] based on a temperature-dependent Thomas–Fermi model, with some modifications on the evaluation of the electron velocity distributions. The bound-electron components ($n_{eb}(r)$, $v_{eb}(r)$) and the free-electron components ($n_{ef}(r)$, $v_{ef}(r)$) were separately evaluated.

For calculation concerning the projectile, in order to take into account the translational motion, we used an effective temperature kT_{eff} given by

$$kT_{eff} = \left(\frac{v_{th}^2 + v_p^2}{v_{th}^2} \right) kT \tag{4}$$

instead of the ambient temperature kT. In the formula above, v_{th} is the thermal electron velocity in the target given by $(3kT/m)^{1/2}$.

The above calculations were performed for $Z_1 = 28$ (Ni) projectiles and $Z_2 = 18$ (Ar) target with atomic densities $n_{atom} = 10^{19}$–$10^{23}\,cm^{-3}$ and temperatures ranging from the room temperature to $\approx 10^5$ K.

3. Results and discussion

3.1. Radial electron distributions

An example of calculated distributions of the electron density and the mean electron velocity in a target atom is shown in Fig. 2. The Wigner–Seitz radius given by $R_{WS} = (3n_{atom}/4\pi)^{1/3}$ is 6.2×10^{-8} cm. At $r = R_{WS}$, continuity and discontinuity are observed for the distribution of free and bound electrons, respectively. In this case, the